Chapter 6
Vacuum Mechanisms of Nanoscale Precision

The principles of design of vacuum mechanims of nanoscale precision are presented. Physical basics of the mechanisms nanoscale precision are discussed. Vacuum multicoordinate drives and manipulators are also shown.

The analysis of vacuum technological equipment and vacuum research equipment shows that the most strict requirements for the object transference are in electron beam micro lithography equipment. For example, electron beam micro lithography installations with work pressure $p = 10^{-5}$ Pa must ensure the positioning error is below 0.5–1.0 mic. The total error of instrument (and coordinate table) [1] positioning in this installation is below 100 nanometers. Even higher requirements are in X-ray lithography installations which use synchrotron source as a work beam [2]. In the process of sample transference this equipment requires that the silicon water inclination from the base X-ray sample should be below 20 nanometers. These high requirements are caused by the work beam inclination. In the X-ray installations, the work beam is not inclined by the electric field as in the electron beam lithography. In new research equipments: in the ultrahigh vacuum scanning tunneling microscopy installations, in atomic force microscopy, the error of the instrument transference must be less than 0.1 nanometer (at a work pressure $p \leq 5 \cdot 10^{-8}$ Pa) [3].

The other types of research equipment, for example ultralarge segmented astronomy telescopes equipped with an adaptive optical system, requires small positioning error less than 50 nanometers. This system also has special requirements on cleaniness and absence of debris (products of wear) [4]. This equipment requires also very quick action of the drive (the time of action is less than 10^{-1} micro-second). It is related with the necessity of high productivity and multi-step transference of

E.A. Deulin et al., *Mechanics and Physics of Precise Vacuum Mechanisms*,
Fluid Mechanics and Its Applications 91, DOI 10.1007/978-90-481-2520-3_6,

the sample with high precision. The quick action of the drive can be achieved with the high stability of the motion of the drive: the equipment requires short time decreasing of the transference process as well as high speed of sample transfer [5]. To ensure nanometer precision in combination with millisecond quick-action of the drive, it is necessary to use the correct type of the drive and to have a system with computer control. For this task it is necessary to establish the principles of transference of ultrahigh precision of vacuum mechanisms.

6.1 The Principles of Nanometer Precision of Vacuum Mechanisms

It was shown in Chapter 5 that only loop-controlled vacuum mechanisms are able to limit the number of positioning errors. It was shown [5] that the total positioning error of loop-controlled drive which works in a stable environment can be expressed by Equation (5.10):

$$\delta\varphi_\Sigma = \delta_V + \delta_N + \delta_{CT},$$

where δ_V is the error of driving action variation (this error is determined by the drive structure and by the drive control system); δ_{CT} is the static error of the drive (this error is limited by the static friction forces in the drive elements and by the measuring system).

Let us consider the total error $\delta\varphi_\Sigma$ components of the drives of nanometer scale. The error of driving action variation δ_V can be expressed by the following equation [5]:

$$\delta_V = C_0\varphi + C_1\omega + C_2\varepsilon, \tag{6.1}$$

where C_0, C_1, C_2 are the errors coefficients: positioning coefficient, speed coefficient, acceleration coefficient, respectively; φ, ω, ε are the drive coordinate, drive speed, drive acceleration, respectively.

In the drive static control system (at a static level $\nu = 0$) the drive error of driving action variation $\delta_V = C_0\varphi$. The drive static control system which contains one integrant element ($\nu = 1$), the positioning error is equal to zero ($C_0 = 0$) and the δ_V error of driving action variation component depends on dynamic error:

$$\delta_V = C_1\omega = \omega/k_\Pi,$$

where k_Π is the common speed transmission coefficient of automatically controlled drive.

In the case of the static system containing two integrant elements, the positioning and speed errors are equal to zero ($C_0 = C_1 = 0$) and δ_V error of driving action variation depends on the acceleration error $\delta_V = C_2\varepsilon$.

In the presence of disturbing forces (F_{dist}) (technology forces variation, vibration of base forces, atmosphere pressure forces variation after the vacuum chamber opening, energy variation and hydraulic pumping station variation), the error [5]

Table 6.1 Parameters of transference measuring systems.

Technical parameters of transference measuring systems	Photoelectric sensor of linear transference (Model BE-164, ENIMS, Russia)	Inductive sensor of of positioning (WS100D ... WS600D, HBM, Germany)	Industrial laser interferometer (HP5528A, Hewlett Packard, USA)
Range of the transference length, m	1.02	0.6	60
Precision of transference measurement, Nm	500	100	10
Maximum speed of transference, m/min	10	–	18

appears:

$$\delta_N = F_{\text{dist}}/(k_{\text{damp}} i^2 k_a), \tag{6.2}$$

where k_{damp} is the damper coefficient of the drive; i is the coefficient of the drive transmission; k_a is the common amplifier coefficient of open control system of the drive.

When using vibro-isolated base units and thermostatic systems as well as in the case of hydraulic pumping stations of high stability, the error δ_N can be reduced to a small value ($\delta_N = 0$). The "static" error δ_{CT} of loop-controlled drive can be determined by Equation (5.11).

This error is caused by a dead zone of the loop-controlled drive. It can be presented as

$$\delta_{CT} = \delta_c + \delta_L + \delta_I \quad \text{(Equation (5.11))}$$

where δ_c is the error component caused by friction forces and other resistance forces (friction forces, elastic forces and pressure forces of sealing bellows and membranes, etc.); δ_L is the error component caused by recoil (gap in a kinematic chains); δ_I is the instrumental error component which is determined by the accuracy rating of a sensor as well as by a zero drift of the amplifier.

Precise vacuum drive must consist of parts (motor, transmission, pilots) without recoil elements. The recoil decreasing in kinematic chains of transmission leads to an increase of the friction force and an increase of the error component δ_c. The use of hydraulic or piezo electric drive elements helps to remove the recoil component ($\delta_L = 0$).

The different types of measuring systems: raster grids, inductive sensors, laser interferometers are used for drive transference measurement. Table 6.1 shows the parameters these measuring systems.

We can see that vacuum equipment (for example, micro lithography installations) requires the transference at nanoscale precision and it must be equipped with a laser interferometer sensor, which has the transference error $\delta_I = 10$ nm.

In case of higher precision (in the range $\delta_I \leq 0.1$ nm), which is used in scanning tunneling microscopy, the designers use measurement of tunneling current between

the instrument and the sample. The tunneling variation is used to determine the distance between the instrument and the sample [3].

The transference error δ_c of the drive can be expressed as a function of static friction force according to the equation presented in Chapter 5 (see Equation (5.13)):

$$\delta_c = F_{CT}/k_0,$$

where k_0 is the drive transmission coefficient in static friction force; F_{CT} is the static resistance force in the drive (in motor, chains of transmission, in pivots).

Static resistance force of vacuum equipment is formed not only due to surface friction, but also as a result of the weight of transported objects, atmospheric pressure, and elastic forces which can be as high as hundreds of Newtons.

At the beginning of a motion, a dead space of follow-up system (error δ_c) can be determined by Equation (5.13):

$$\delta_c = I_{TP}/(k_D \cdot k_y),$$

where I_{TP} is the steering command (starting current on the drive input which corresponds to the beginning of the drive movement); k_D is the transmission coefficient of the positioning sensor; k_y is the amplifier coefficient of measuring system.

The theory of follow-up system [5] shows that dead space δ_c of any type of the drive is determined by the starting current (I_{TP}) of the follow-up system and by the common transmission coefficient of the measuring system:

$$k = k_D \cdot k_y.$$

In case of a constant motor control current the higher amplifier coefficient corresponds to a lower positioning error, but in this case the stability of the control system can be changed.

For determining the optimal value of the coefficient $k = k_D \cdot k_y$ it is necessary to create the dynamic model of the drive control [5] which should be stable, of high quality, and very precise.

The analysis of the total positioning error components of mechanisms of a precise vacuum drive shows that the most influence on the transference error is in the static error δ_{CT} of the drive, also as in the error δ_c as a result of static friction force in the drive.

As a result of different types of the drive analysis, of the matrix analysis, of the matrixes of the drive structure and of the drive design, the drive composition and drive structure variants were classified according to two main parameters: precision of transference and quick-action of the drive.

These parameters are: "static friction force" which determines error δ_c and which acts in the motor (see Figure 6.1), pilots (see Figure 6.2) and in vacuum sealing elements (see Figure 6.3).

The "type of the drive" parameter determines quick-action of the drive, see Figures 6.1 and 6.3.

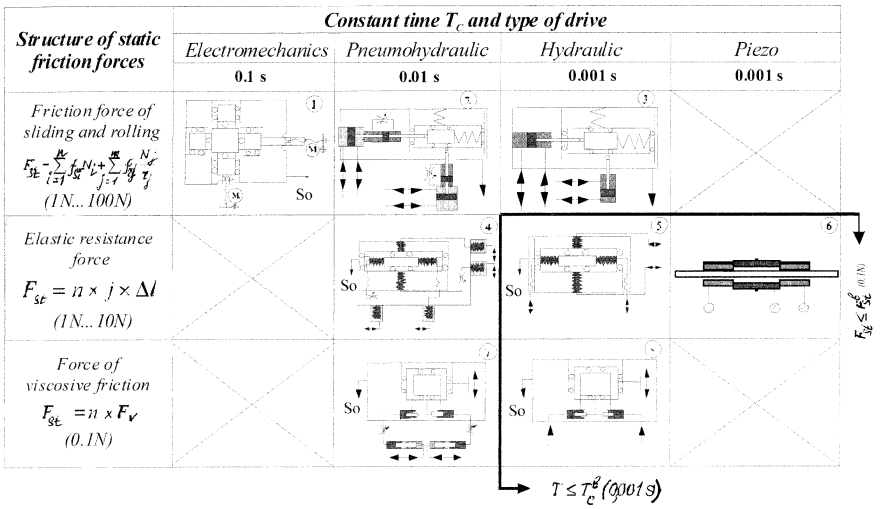

Fig. 6.1 Analysis of the precise vacuum mechanisms by parameters: "type of drive" and "static friction force in the drive".

Apart from this, the drive pilots are analyzed by the parameter "Number of movement degrees" as it is shown in Figure 6.3. In technological and in research equipment it is necessary to move the object in three or more coordinates.

Let us analyze different kinematic schemes of the drives which can be used in vacuum technological equipment, in research vacuum equipment or in other equipment which is estimated by clean technological media where the drive only meets minimal friction forces and can ensure maximal rigidity of the elements of the kinematic chain.

As is known from the theory of automatic control [6,7], hydraulic, pneumatic and pneumohydraulic drives have the best dynamic parameters. Nevertheless, historically in the beginning of vacuum equipment development, the first vacuum equipment was equipped with an electromechanical drive which had base elements operating in vacuum.

The electromechanical drives are usually supplied with long multi-element kinematic chains. These chains consist of motor, sockets, reduction gears, transmission, sealing elements (vacuum motion feedthroughs) [6]. The presence of long kinematic chains leads to decrease of its rigidity and decrease in kinematic and dynamic precision [6]. Electric motors of such drives cannot be used inside vacuum chambers of such installations without additional sealing elements, because of high level of electromagnetic fields, bad vacuum sealing and high level of the outgassing flow. The additional sealing elements and electric motor protection leads to an additional length of the kinematic chain.

Let us analyze different kinematic schemes of the drives (see Figure 6.1) using the parameter "structure of static friction force in the drive".

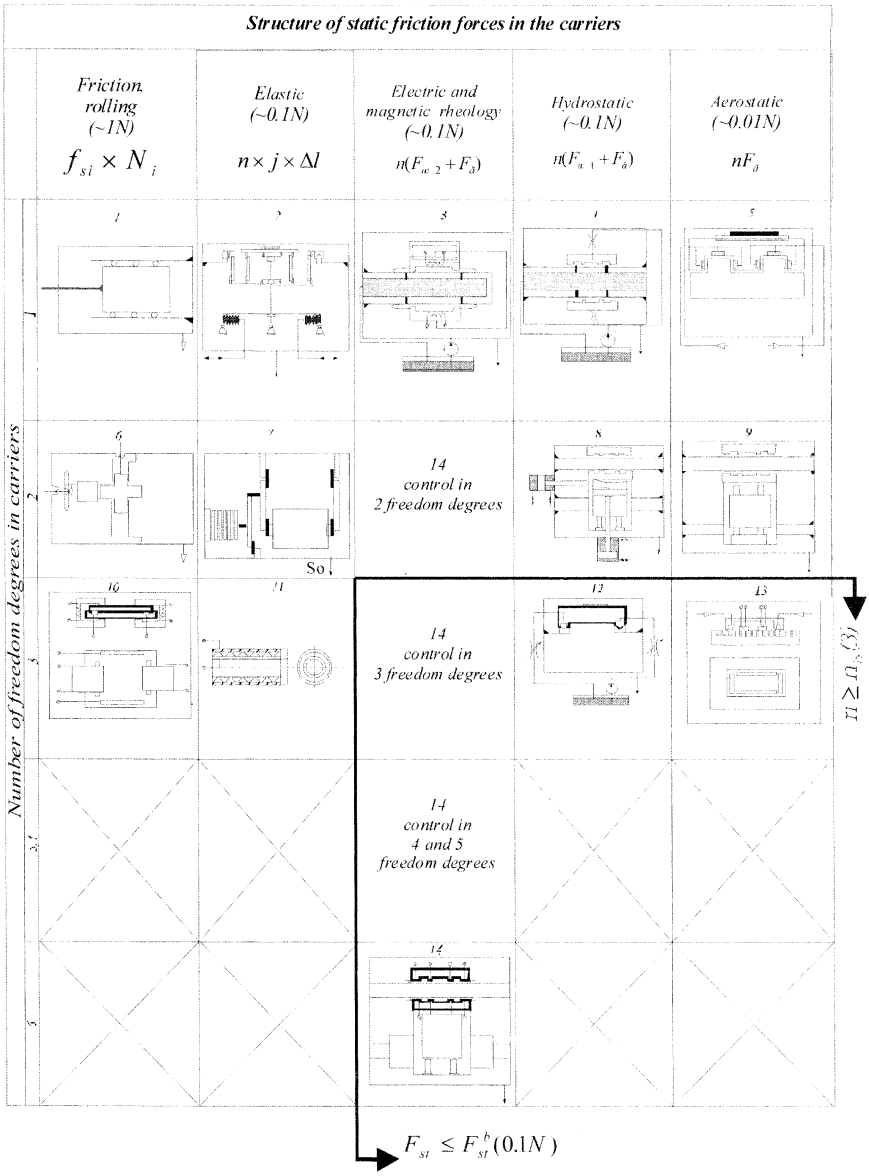

Fig. 6.2 The precision vacuum mechanisms analysis using the parameters: "static friction forces in the carriers" and "number of freedom degrees in the carriers".

Scheme 1 in Figure 6.1 shows the electromechanical drive of an electron beam lithography installation in which the drive is based on a stepper motor. The motion of the stepper motor goes through gear pairs, nut-screw pairs to low and to high

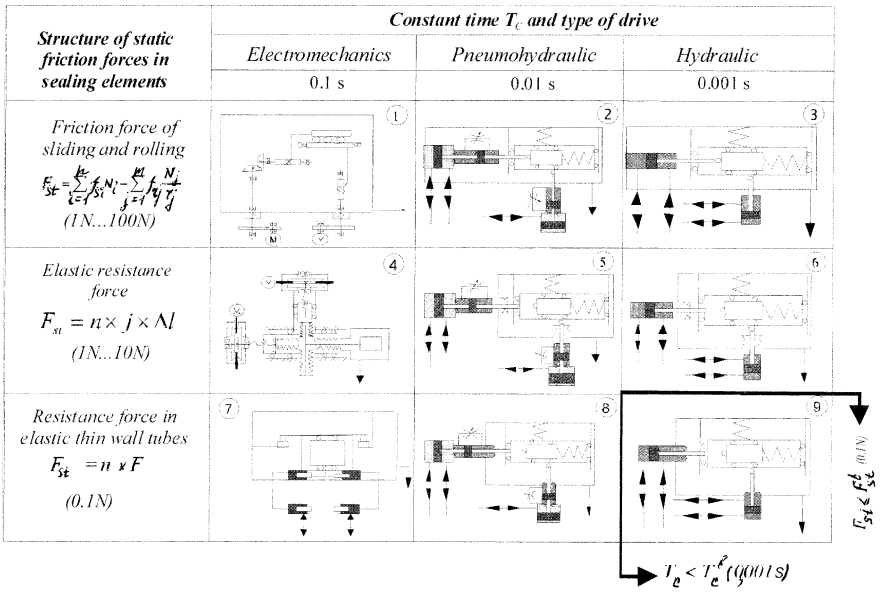

Fig. 6.3 Analysis of the precise vacuum mechanisms by parameters: "constant time T_c and type of drive" and "static friction forces in sealing elements".

pilots of coordinate table in vacuum. Thin-wall elastic sockets are used as sealing elements.

The schemes 2 and 3 show the pneumohydraulic drive and hydraulic drives based on "cylinder-piston" pairs and based on stuffing box seal type. Static friction forces appear in the seals of hydrocylinders. Furthermore, these schemes show the pneumohydraulic drive and hydraulic drives based on welded bellows.

The pneumohydraulic drive (scheme 4) consists of four welded bellows connected by pairs of tubes which are filled in by work liquid. In every pair of bellows one bellow is situated inside pneumatic germetic volume of cylinder. Resistance force in the drives 4, 5 (schemes 4, 5) appears because of the deformation of welded bellows and this force varies in value and in direction in the process of coordinate table movement. Scheme 6 shows a stepper piezo drive, which contains three piezo tubes. Resistance force of the drive appears in the middle piezo-tube in the process of its axial deformation.

Schemes 7, 8 show the variants of pneumohydraulic (7) and hydraulic (8) drives, which use thin-wall rubber socks.

In case of precise transference, the high requirements are not only on the motor, but also on pilots which as a transference base, have a great influence on the precision of the transference. The pilots of a high precision drive must comply with the following requirements:

- low friction;
- high rigidity;

- absence of recoil;
- high smoothness of the transference;
- high wear protection;
- compatibility with vacuum and other clean conditions;
- technology protection.

The design and creation of pilots which meet all of these requirements is a difficult task. In the realization of this task the designer often creates the best technical variants but these variants often compete with other requirements, and for example the designer has to use non-recoiling pilots with small friction force but with low rigidity.

In the mechanisms of high precision all types of pilots can be used as shown in Figure 6.2: friction, rolling, elastic, hydrostatic, aerostatic.

The most often used variants are the rolling (scheme 1) and the friction one (scheme 6 corresponds to electron lithography installation), which corresponds to the sample transference in one, two, or three direction [8]. The rolling type pilots correspond to small friction forces, small differences between static and dynamic friction force, high rigidity and high precision in all directions of the transference. Nevertheless, this type of pilots has high cost (price) and increased in its manufacturing, it has also small damping ability in the direction of the motion. Movable friction pilots were not used in vacuum technology till recent time. New materials and new technology can help designers of electronic technical equipment to decrease the manufacturing costs of this type of pilots and to increase the damping ability.

The success of manufacturing of friction-type pilot depends on ceramic materials, new technology, and new antifriction coatings. In engineering, designers use pilots supplied with combined facets of rolling and friction transference. Rolling facets are situated in the direction of maximum load. The other ones are covered with antifriction coatings or use Teflon coatings combined with hardened steel. This variant increases the rigidity of this type of pilot from 1.5 to 3 times in comparison with rolling type pilots. This type of pilot has lower resistance forces 4 to 7 times in comparison with friction type pilots and better damping properties. Scheme 2 shows the elastic pilot with one degree of freedom for electron beam lithography installation. The schemes 7 and 11 show piezo electric mechanisms of elastic pilots, the mechanisms of high precision transference in two and in three directions. The use of hydrostatic and aerostatic pilots is limited because of bad properties which cannot be used in vacuum and clean technological conditions. Good properties of this pilot (no recoil, small friction forces, smooth movement, high precision) should be accompanied by good sealing properties of these pilots. Scheme 4 shows the hydrostatic pilot (of cylinder form), which can be used in coordinate table drive for electron beam micro lithography installations. Scheme 8 shows two coordinate table for electron beam lithography which is supplied with hydrostatic pilots of cylinder shape. Scheme 12 shows hydrostatic pilot of one coordinate measuring system [9], which is supplied with electrohydraulic transformers which allow the realization of microtransference in vertical direction and in rotation around a horizontal axis.

These microtransferences are used for precise positioning. Scheme 3 shows hydrostatic pilot design based on magnetic rheology phenomena [10, 11]. In this design the magnetic rheology suspension is used as a work liquid. This pilot has all advantages of hydrostatic pilots:

- low friction force,
- high precision,
- high smoothness of transference,
- good damping properties,
- high rigidity,
- absence of recoil.

Active throttling of a magnetic rheology liquid helps to realize radial micro transference of a pilot body within limits of radial gaps of the pilot. The pilot sealing is realized using thin-wall rubber socks. Scheme 14 shows a two-coordinate table equipped with electro-rheology throttling of work liquid [10]. As a work liquid of this pilot an electro-rheology suspension is used.

The number of motion freedom degrees of this pilot is determined by a control system and this number can range from one to six.

Schemes 5 and 9 show one- and two-coordinate tables based on aerostatic pilots for installations of photolithography. Scheme 13 shows the coordinate table pilot which is used in photolithography installation [12] and which is based on the linear stepper motor. The table is transferred in two coordinates and is based on an air cover which is fixed on a flat plate which can be rotated on a plate surface.

A vacuum drive must produce a minimum outgassing rate of gases in a vacuum chamber or in a chamber with clean technological media. Different types of sealing elements with different structure of resistance force are used for this purpose. Let us analyze the precise vacuum drive on parameter: "Resistance forces caused by sealing elements". Scheme 1 (see Figure 6.3) shows the electromechanical drive based on throttle motors. Vacuum rotary-motion feedthrough is based on two vacuum rubber cuffs. The rotation motion is transformed into linear motion using the "shaft–roll" friction pair. Scheme 2 shows the variant of pneumo-hydraulic drive of electron beam lithography installation. The pistons and rods of pneumo hydraulic cylinders are sealed in this installation by cuff seals. Scheme 3 shows the drive in which cylinder rods are sealed by cuff seals. These drive schemes are determined by the work liquid evaporation into vacuum chamber and this contaminates the elements of electron optical system. Scheme 4 shows the electro mechanical drive of electron beam lithography installation. The drive sealing is realized by metal bellows which are protected from atmosphere pressure by T-form element. Schemes 5 and 6 show the variants of pneumo-hydraulic (Scheme 5) and hydraulic drive (Scheme 6) in which welded bellows protect the system from the vapors of work liquid. Scheme 7 shows the electromechanical drive based on four hydro-cylinders sealed by thin-wall rubber socks. The pairs of hydro-cylinders are connected by tubes. Schemes 8, 9 show the variants of pneumo-hydraulic (Scheme 8) and hydraulic drive (Scheme 9) in which the hydro-cylinders are sealed by thin-wall rubber socks.

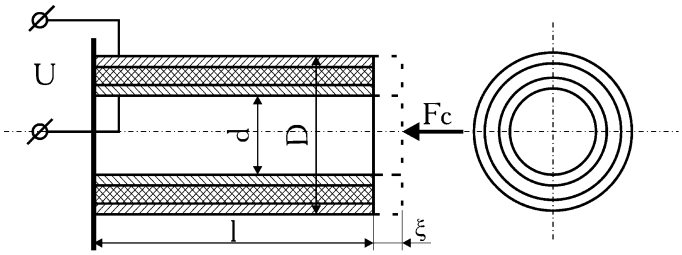

Fig. 6.4 Scheme of piezo tube drive.

As we can see, the analysis of different types of pilot and different types of sealing elements forms the basis for selection of optimal designs and structures of precise vacuum drives (Figures 6.1, 6.2, 6.3). The zones of optimal structural solutions of the drive are shown in the tables by arrows. The arrows point to some technical parameters: time constant T_Π, (the pointed drive parameter in which T_Π is less than 1 millisecond), static resistance force F_{st} (the pointed drive parameter in which F_{st} is less than 1 N). As we can see points show the zones of tables where the drives of high positioning precision are situated.

6.2 Physical Effects Which Are Used for Vacuum Mechanisms of Nanometer Precision Creation

6.2.1 Piezo Effect

Analysis of literature and patents [13–15] allows one to find piezo transformers which can be used for vacuum mechanisms of nanometer precision.

These mechanisms can be characterized by the properties:

- error of transference below ± 10 nm (nanometers),
- high smoothness of transference,
- high sensitivity,
- high speed action (time constant below 2 microseconds),
- possibility of reversed transference,
- absence of heat generation at work.

The range of piezo drive transference is less than 400 mic. Piezo transformers can be used to perform two types of motion: transversal and longitudinal. Let us consider two corresponding schemes of piezo transformers: tube and column.

For the tube scheme, the transference of the end of the drive shown in Figure 6.4 can be expressed [15]:

$$\xi = 2d_{31}lU/(D-d) - 4S_{11}lF_c/(\pi(D^2-d^2)). \tag{6.3}$$

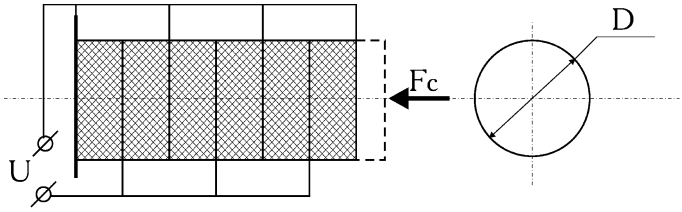

Fig. 6.5 Scheme of piezo column drive.

For the column scheme, the transference of the drive shown in Figure 6.5 can be expressed as [15]:

$$\xi = nd_{33}U - 4nS_{33}hF_c/(\pi D^2), \tag{6.4}$$

where d_{31}, d_{33} are the parameters of piezo modules corresponding to effects of cross and longitudinal deformation as a result a unit electric field m/v; l, h, d, D are the size parameters of tube and column, m; n is the number of disks in the piezo column; U is the input voltage of piezo drive, V; S_{11}, S_{33} are the backward modules of elasticity of piezo materials of tube and column; F_c is the external load, N.

The size of longitudinal piezo module d_{33} is two-fold larger than d_{31} of cross piezo module [15].

The maximum force of piezo tube $F_{c\max}$ (Figure 6.4) [15] can be expressed as

$$F_{c\max} = \pi d_{31}(D + d)U/(2(S_{11})^E). \tag{6.5}$$

The maximum force of piezo column $F_{c\max}$ (Figure 6.5) can be expressed as

$$F_{c\max} = \pi d_{33}D^2U/(4(S_{33})^E h). \tag{6.6}$$

The designers usually use piezo ceramics for piezo drives. Usually this ceramic is of the ZTP type which consists of Zr, Ti, Pb. These components have the highest piezo activity, high time stability of properties, high stability of electric load. The graph of the drive transference $X = f(U)$ (Figure 6.6) shows hysteresis which is typical for the piezo electric drive. As an example of a piezo drive let us consider a drive based on a piezo column supplied with a reduction mechanism [15]. The scheme of this drive and its main parameters (transference X of output part of the drive, piezo column deformation ξ) are shown in Figures 6.6 and in 6.7.

Figure 6.7 shows a piezo column of active length $l_A = 50$ mm which is made of ZTP piezo ceramic. It consists of discs of diameter $D = 18$ mm and thickness $h = 1$ mm. The length of the column transference is $X = 200$ mic. The voltage of input current is $U = 600$ V.

Piezo drives parameters can be described by the "after effect" which can be described by deformation of piezo element increasing at constant electric load. For example, the drive shown in Figure 6.7 reaches deformation of piezo drive about 1 ... 2.5 mic after applying constant voltage U during a time period of about 4

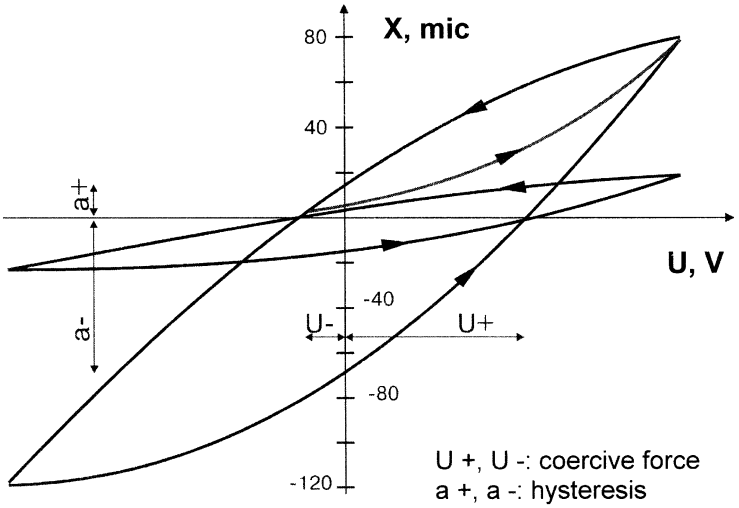

Fig. 6.6 The piezo column deformation (output element transference) X (mic) as a function of input voltage U. The symbols on the graph U^+, U^-: coercive force, a^+, a^-: hysteresis.

minutes, as shown in Figure 6.8. This effect can be removed by increasing voltage on the piezo drive.

6.2.2 Magnetic and Electric Rheology Effects

Magnetic and electric fields in cross-section of a tube (throttle) (see Figure6.9) filled with magnetic (MR) or electric (ER) rheology suspension lead to quick variations of dynamic viscosity of these suspensions (see Figure 6.10). These effects can be used for design of magnetic and electric rheology throttle (MR and ER throttle). This design helps to remove traditional for hydraulic design controlling elements: valves, slide membranes, screens. These factors allow one to decrease the service life of a throttle. The time period is less than 1 millisecond for a magnetic rheology throttle and less than 0.1 millisecond for an electric rheology throttle because of the elimination of inertia elements.

As a work liquid in these throttles magnetic rheology (MR) and electric rheology (ER) suspensions can be used. These suspensions can be considered as a dispersed physical-mechanical system consisting of two (liquid and solid) phases separated by a large surface. One of the phases (dispersed phase) is distributed in size of the particles from 10^{-3} to 10^{-2} mm.

As a dispersed magnetic rheology phase, the designers use microparticles of Fe and CrO_2 or microparticles made of other soft magnetic materials. As a dispersed

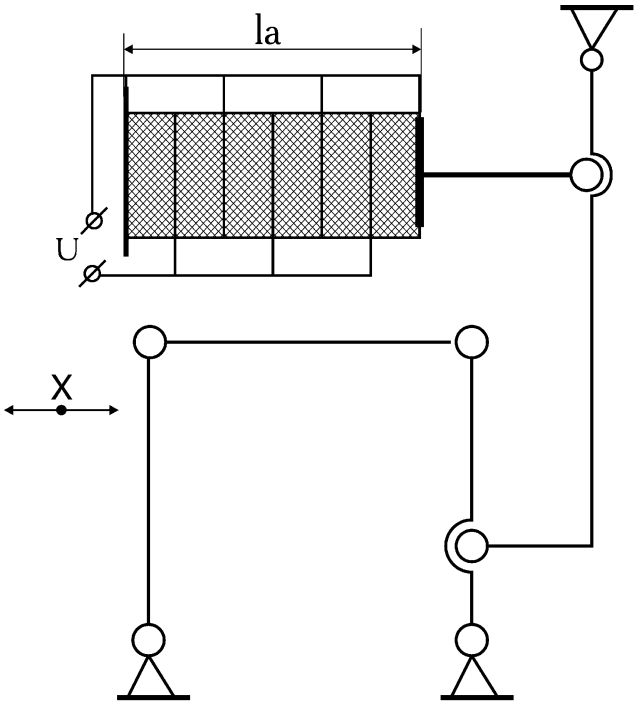

Fig. 6.7 Scheme of piezo drive supplied with reduction mechanism.

electric rheology suspension microparticles of SiO_2 can be used. As a dispersed phase vacuum oil can be used.

The stream of magnetic rheology (MR) suspension can be described by Newton's flow laws [16] with Newton behaviour parameter n. In absence of a magnetic field in the zone of low suspension speed, the flow of magnetic rheology suspension corresponds to pseudo-plastic law:

$$\tau = k \cdot \dot{\gamma}^n, \tag{6.7}$$

where τ is the shearing stress; k is the consistence of magnetic rheology (MR) suspension; γ is the shearing velocity; n is the parameter of magnetic rheology suspension in Newton behaviour.

Under external magnetic field, a magnetic rheology suspension changes its viscosity: thre are plastic properties [16, 17] in the area of low shearing velocities with behaviour corresponding to the Balkly–Gershel law:

$$\tau = \tau_0 + k \cdot \dot{\gamma}^n, \tag{6.8}$$

where τ_0 is the viscous flow limit which depends on external magnetic field, material, volume concentration of dispersed phase and magnetic rheology suspension

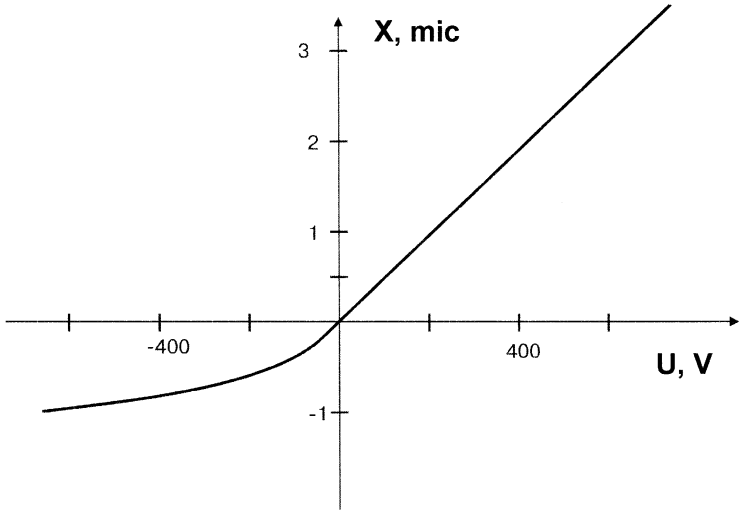

Fig. 6.8 Diagram shows "after effect" of piezo drive; the symbols on the graph: X – column transference (mic), U – constant voltage (V).

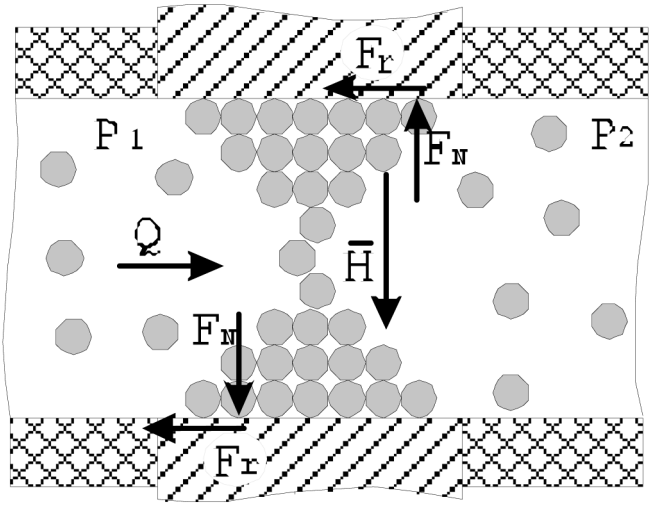

Fig. 6.9 Scheme of work gap of magnetic rheology throttle.

temperature; k is the consistence of magnetic rheology (MR) suspension, which is similar to plastic viscosity of work liquid.

We can see from Equation (6.8) that shearing stress τ depends on shearing velocity. This dependence corresponds to non-linear law. To simplify the engineering calculations of a precise hydro-drive based on magnetic rheology suspension as well

as to use the automatic control methods of a hydrodrive, it is necessary to consider a magnetic rheology suspension as a Newton liquid described by Newton behaviour, which is equal to one. It is necessary also to use the term "equivalent dynamic viscosity". According to Ichibara [8], the term "equivalent dynamic viscosity" corresponds to viscosity of Newton liquid whose flow is equal to abnormal viscous liquid.

Equation (6.8) of shearing velocity $\gamma \neq 0$ in this case can be presented as

$$\tau = \mu_{\text{eqv}} \dot{\gamma}, \tag{6.9}$$

where μ_{eqv} is the "equivalent dynamic viscosity" of magnetic rheology suspension.

It is known that Newton liquid flow is described by the linear equation (6.9) if the liquid flow is layered. The critical value of Reynolds number (flow laminarity must be less than Reynolds number) usually corresponds to [18]

$$\text{Re} = u \cdot h/\nu = 1000 \ldots 1200, \tag{6.10}$$

where h is the work gap for magnetic rheology throttle; u, ν is the flow speed and kinematic viscosity coefficient of work liquid (magnetic rheology suspension). The Reynolds number is less than 10 in magnetic rheology hydrodrive. This factor ensures layered flow of work liquid.

In our case "equivalent dynamic viscosity" μ_{eqv} of magnetic rheology suspension or electric rheology suspension can be considered as a function of the following parameters: magnetic field strength H or electric field strength E, temperature t (°C), volume concentration of dispersed phase of micro particles φ_v and dynamic viscosity μ of dispersed phase. The graphs of "equivalent dynamic viscosity" μ_{eqv} of magnetic rheology suspension based on carbide Fe particles and graphs of "equivalent dynamic viscosity" of electro rheology suspension based on SiO_2 particles as a function of magnetic field strength H or electric field strength E [8] are shown in Figure 6.10.

The dispersion medium in both examples is vacuum oil VM-4 (Russian standard). The temperature of suspension is constant in both cases and is equal to $t = 30$°C. The volume concentration of micro-particles of dispersion phase is

$$\varphi_v = V_P/(V_P + V_M),$$

where V_P, V_M are the volumes of microparticles (V_P) and of oil (V_M) which are collected for magnetic rheology suspension at field strength: $\varphi_v = 0.2, 0.16, 0.12$ and for electric rheology suspension at field strength $\varphi_v = 0.2$.

Graphs of equivalent dynamic viscosity $\mu_{\text{eqv}}(H, E)$ (Figure 6.10) can be divided into three parts. The first two parts of the graphs can be described by the equations: $\mu_{\text{eqv}}(H, E) = A_0 + A_1 \cdot H(E)$, where A_0, A_1 are the constant coefficients. It can be used for the drive control because of good linear properties of the parameters. The third part of the graph is described by the large variation of $\mu_{\text{eqv}}(H, E)$ and after magnetic field strength H or electric field strength E reach the strengths values H_S or E_S (Figures 6.10b, a) the rigid "cluster membrane" is created at the gap of the

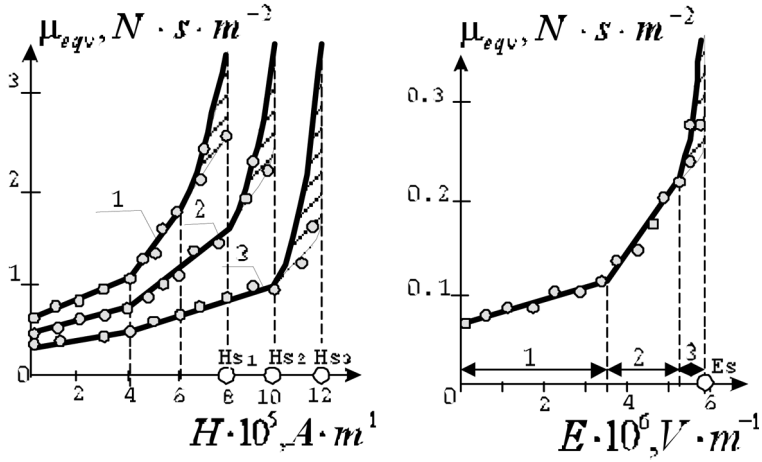

Fig. 6.10 Graphs of equivalent dynamic viscosity μ_{eqv} as a function of field strength in work gap; (a) for magnetic rheology suspension (1: $\varphi_v = 0.2$; 2: $\varphi_v = 0.16$; 3: $\varphi_v = 0.12$); (b) for electric rheology suspension ($\varphi_v = 0.2$).

throttle. This membrane shuts down the throttles based on magnetic rheology or electric rheology.

The expenditure of work liquid in throttles of magnetic rheology or electric rheology during the work process which corresponds to the first two parts of the parameter $\mu_{\text{eqv}}(H, E)$ variation can be expressed as

$$Q = (P_1 - P_2)S^3 b/(12\mu_{\text{eqv}}(H, E)L), \tag{6.11}$$

where P_1, P_2 are the input and output pressure of work liquid of magnetic rheology and electric rheology throttles; S is the value of work gap; b is the width of the gap in cross direction which is normal to the flow of the work liquid; L is the length of the gap in the direction of flow of the work liquid.

6.3 Vacuum Drives and Manipulators of Nanoscale Precision

Matrix analysis of vacuum mechanisms (see Section 6.1) allows one to find optimal structure schemes of the drives which can provide high precision, quick action, good vacuum parameters. Let us consider the design and the work of these mechanisms: piezo drives, magnetic and electro rheology drives and manipulators.

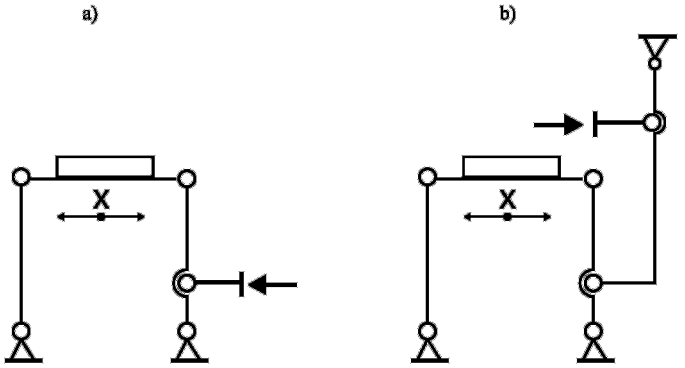

Fig. 6.11 Kinematic schemes of piezo drive of linear transference supplied with lever-multiplication system: (a) one-step system; (b) two-step system.

6.3.1 Vacuum Piezo Drives

Let us consider piezo drive based on a piezo column [15] supplied with a reductor mechanism. The scheme of the drive and its parameters: output element transference X, piezo column deformation ξ are shown in Figures 6.6, 6.7 and 6.8. Piezo column with active length $l_A = 50$ mm is made of piezo ceramic of ZTP type. The column consists of discs of diameter $D = 18$ mm and thickness $h = 1$ mm.

The piezo drive based on piezo tube [14] is used for instrument transference on three orthogonal coordinates X, Y, Z in the system of scanning microscopy.

The method presented in [15] allows one to calculate electrical parameters and design parameters of piezo drive and to providce the required output parameters of piezo drive.

The output parameters of piezo drive are the following: minimal transference $x_{\min}$ ($\varphi_{\min}$), range of transference $x_{\max}$ ($\varphi_{\max}$) in area of linear and angular coordinates. The calculated parameters are: output parameters of piezo drive ratio i of lever multiplicative system of the drive, active length of piezo element l_a, piezo element input current voltage U. The method of piezo drive parameters calculation includes the following main parts:

1. *Design of kinematic scheme of the drive*
For the required transference of output element (object): $x_{\max} \leq 80 \ldots 100$ mic, $\varphi_{\max} \leq 2'$ a one-step system of multiplication can be used (see Figures 6.11a, 6.12a) at $x_{\max} = 100 \ldots 300$ mic, $\varphi_{\max} > 2'$ a two-step system of multiplication (see Figures 6.11b, 6.12b). The ball and socket joints of lever multiplication systems (Figures 6.11a, 6.12a) must be elastic to remove gap errors.

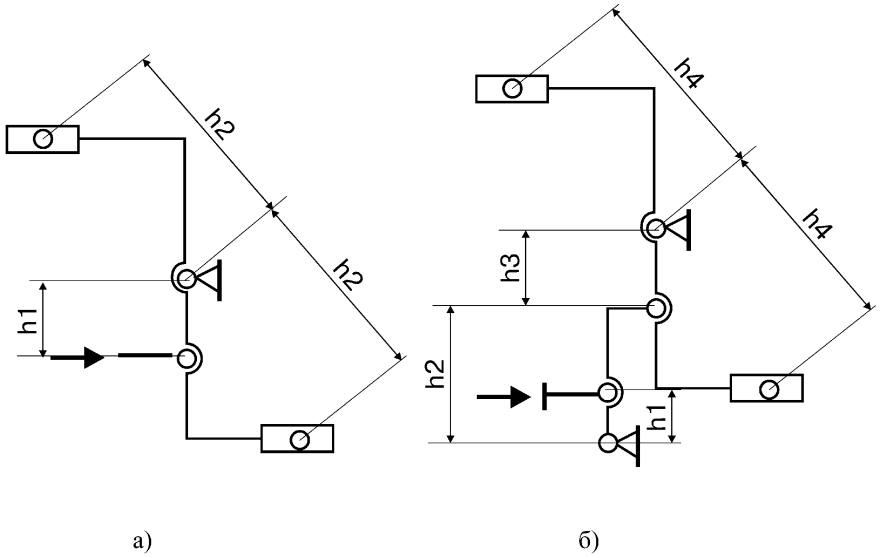

Fig. 6.12 Kinematic schemes of piezo drive of angular transference supplied with lever-multiplication system: (a) one-step system, (b) two-step system.

2. *Determination of multiplication coefficient A and axial rigidity j_Π of piezo element*

For piezo element in the form of piezo column consisting of discs of diameter and height $d = 18$ mm, $L = 1$ mm and made of ZTP piezo ceramic type, the parameters A and j_Π can be expressed as

$$A = 5.4 \cdot 10^{-4} \cdot l_A, \text{ mic/v}, \tag{6.12}$$

$$j_\Pi = 100.4/l_a, \text{ N/mic}, \tag{6.13}$$

where l_a is the active length of piezo element, mm ($l_a = n \cdot h$).

3. *Determination of design parameters of piezo drive*

The multiplication coefficient of a piezo drive is calculated on the base of a given transference range $x_{\max}$ ($\varphi_{\max}$) in linear and angular coordinates. The equation of multiplication coefficient can be expressed as

$$\lambda(x) = x_{\max}/U_{\max}, \text{ mic/V}, \tag{6.14}$$

$$\lambda(\varphi) = \varphi_{\max}/U_{\max}, \text{ mic/V}, \tag{6.15}$$

where $U_{\max}$ is the maximum input voltage, V.

In the case when the maximum input voltage $U_{\max}$ is not fixed it can be adopted in the range of $U_{\max} = \pm 600 \ldots 700$ V.

Then the multiplication coefficient A can be determined as an active length l_a of a piezo element (Figure 6.11b) and a movement translation coefficient (ratio) i.

This coefficient for one-step multiplication system (Figures 6.11a and 6.12a) is $i = h_2/h_1$ and for two-step multiplication system (Figures 6.11b and 6.12b) it is $i = h_2 \cdot h_4/h_1 \cdot h_3$.

4. *Determination of input voltage parameters of piezo drive*
The parameters of constant current of input source are the maximum output voltage $U_{\max}$, discrete of output voltage variation ΔU, output source resistance R_{out}.

$U_{\max}$ parameter determines the transference range of piezo drive. This parameter can be taken from technical conditions or obtained from the drive parameters calculation. The discontinuity of output voltage $U_{\max}$ determines the minimum value of transference.

The discontinuity of output voltage variation $\Delta U_{\min}$ determines the minimum value of transference $x_{\min}$ and can be found from the following equations:

$$(\Delta U_{\min})_x = x_{\min}/\lambda(x),\ \text{V}, \tag{6.16}$$

$$(\Delta U_{\min})_\varphi = \varphi_m in/\lambda(\varphi), \text{V}. \tag{6.17}$$

The output resistance R_{out} of the work current source has an influence on the output current voltage and it can be determined after piezo element connection by

$$R_{\text{out}} = R_\Pi \cdot \Delta x \cdot m/((2 \ldots 4) \cdot 100),\ \text{Ohm}, \tag{6.18}$$

where R_Π is the piezo element resistance at constant current, Ohm (for example $R_\Pi > 10$ MOhm); Δx is the tensile strain of piezo element, %; m is the number of piezo elements connected to the current source.

To ensure precise transference of the objects (which can be for the long travel up to hundred millimeters) in ultrahigh vacuum it is possible to use a step drive based on piezo tubes, e.g. by Burleigh Instruments, Inc. [14]. The scheme of this drive work steps is shown in Figure 6.13.

The control signal in the initial position (scheme a) is not fed to piezo tubes and these tubes are in neutral position. After control signal feeding to piezo tube 1 (scheme b) this tube is reduced in radial direction and it locks the rod. After this the control signal feeds to the tube 2 (scheme b) and this tube increases its length in axial direction. This operation leads to rod transference of one step in left direction.

After control signal feeding to the piezo tube 3 (scheme c), this tube is retracted in radial direction and this tube locks the rod. After this operation control signals of tubes 1 and 2 are eliminated one by one and it leads to width of element 1 increasing. It leads also to back movement of element 2 into initial position (schemes d and e).

After control signal feeding to the piezo tube 1 and signal elimination from the tube 3 (schemes d and e) the work cycle is finished and the drive is ready for the next step. The general view of ultrahigh vacuum step drive on the base of piezo tubes (Burleigh Instruments, Inc.) is shown in Figure 6.14. The general view of the carriage developed on the basis of the above drive is shown in Figure 6.15.

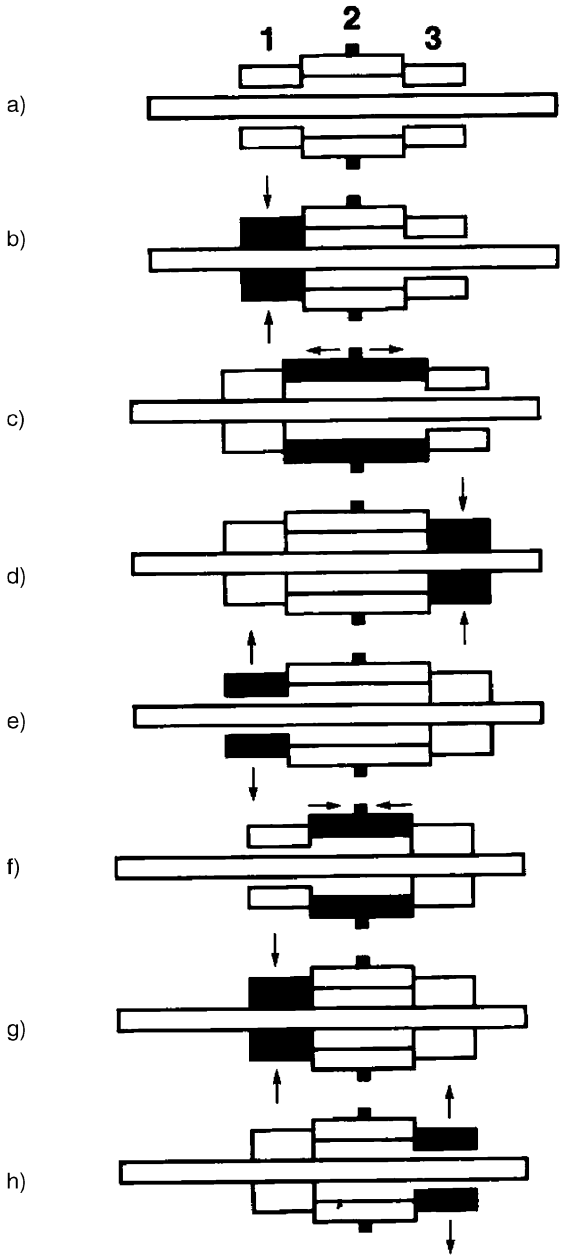

Fig. 6.13 The work stages scheme of step drive based on piezo tubes manufactured by Burleigh Instruments, Inc.

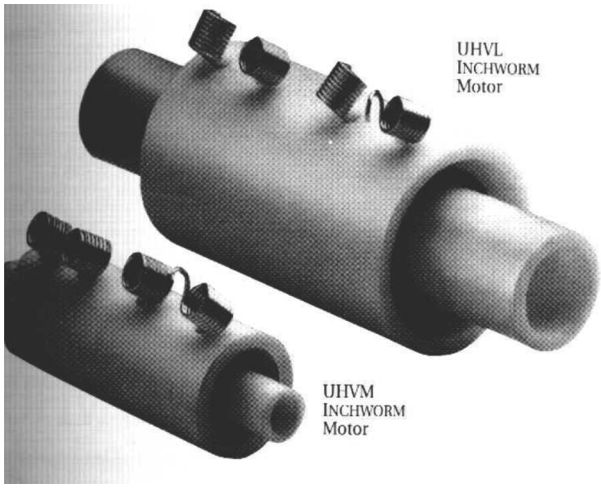

Fig. 6.14 General view of step drive based on piezo tubes manufactured by Burleigh Instruments, Inc.

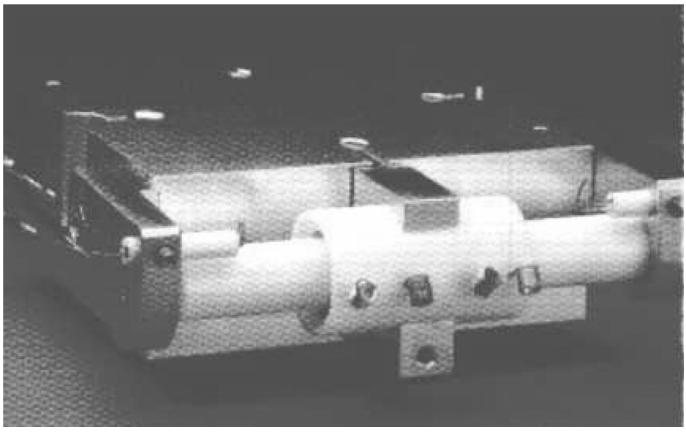

Fig. 6.15 The general view of the carriage which is done on base step drive on the basis of piezo tubes manufactured by Burleigh Instruments, Inc.

6.3.2 Multi-Coordinate Magnetic and Rheology Drives and Manipulators

Let us consider the scheme of a magnetic rheology drive with a large range of transference (up to 200 mm) in one coordinate [19] shown in Figure 6.16. The magnetic rheology suspension based on ferrum carbide and vacuum oil is used in this hydrosystem as a work liquid. The main elements of the drive are the magnetic rheological distributor 4 and thin-wall rubber seals which seal two hydro-cylinders 3

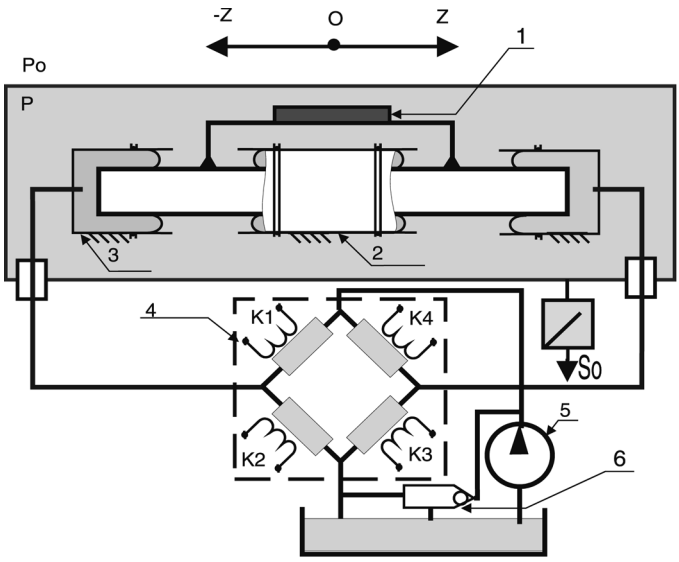

Fig. 6.16 Scheme of long travel magnetic rheology drive.

and guide 2. Magnetic rheological distributor 4 consists of four magnetic rheology throttles containing electromagnet coils $K1$–$K4$ and magnetic field conductors with work gaps for work liquid flow. The transferred object 1, guide 2 and hydro cylinders 3 are situated in a vacuum chamber. The rest of the elements are situated in atmosphere. In case of full shutting of magnetic rheology throttles, the work liquid spills over into a spillage tank through safety valve 6.

The drive works according to the following rules. The work liquid is spilled by the pump 5 from the spillage tank through magnetic rheology distributor into hydro cylinders 3. It is possible to vary the pressure in hydro-cylinders 3 in magnetic rheology throttles using control of dynamic viscosity of work liquid and, thus, it is possible to vary the axial force on the rod. The linear transference is produced in the direction of the Z axis from hydro-cylinders 3 through the rod to the carriage of coordinate table where the transferred object is fixed. In process of rod transference in the direction of the Z axis – inside thin-wall rubber seals 2; these seals roll/move from the rod to the cylinder and back. This seal ensures hermetic sealing of the connection. The general view of the drive is shown in Figure 6.17. The friction guides are used in the drive.

In the case of a small micro transference and under the following conditions: small range (up to 1 mm) of transference, millisecond quick-action, high vacuum research on technological equipment, mirror alignment of inertial mirror elements of high astronomy telescope, the precise magnetic rheology drive [14, 19] of the hydraulic type can be used. The scheme of this drive is shown in Figure 6.18. The hydrodrive consists of hydrocylinder 1, magnetic rheology throttles 2 in tubes, pump 3, sensor of transference 4 and of computer 5. The drive works in the following

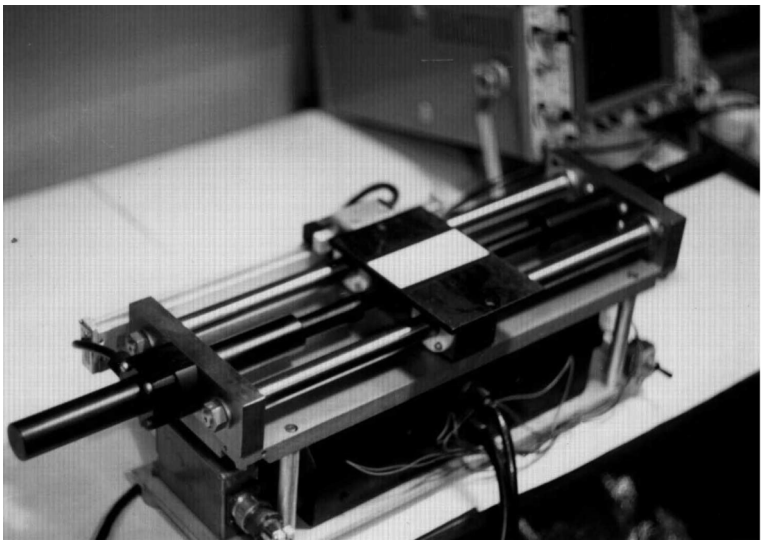

Fig. 6.17 General view of long travel magnetic rheology drive.

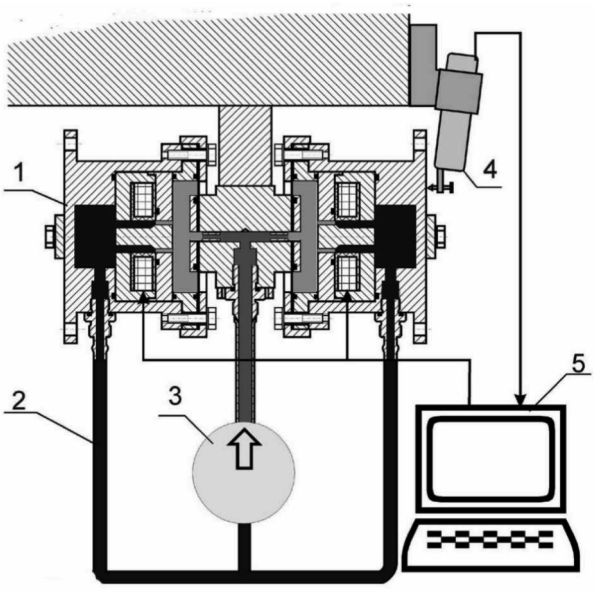

Fig. 6.18 Scheme of one coordinate tuning magnetic rheology drive.

order: work liquid-magnetic rheology suspension is spilled from the pump 3 into the hydrocylinder 1. It is possible to regulate the pressure difference of the work liquid in hydrocylinders 1 and it is possible to vary the object transference along the axis measured by the help of sensor 4.

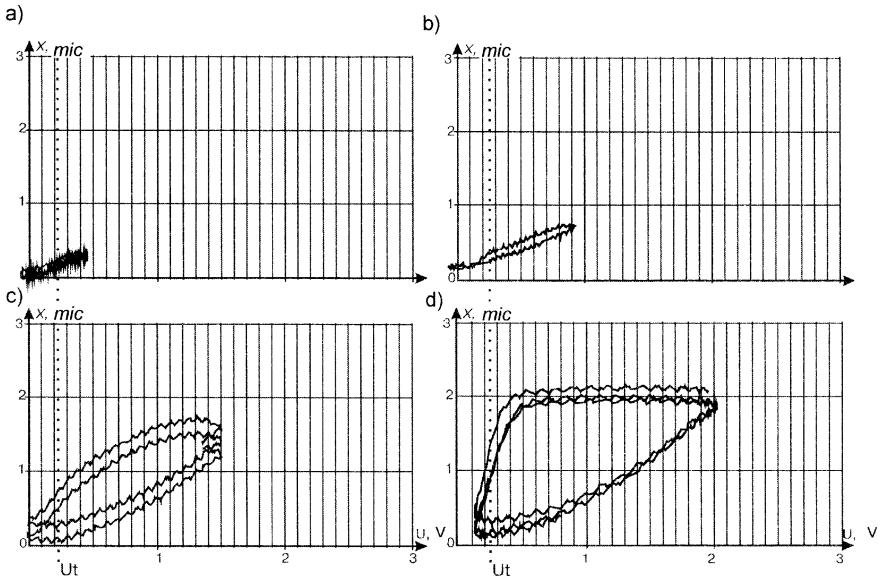

Fig. 6.19 Graphs of transference value X as a function of control voltage U.

The results of the experimental research of precision of a magnetic rheology drive (see Figure 6.18) are shown in Figure 6.19. The scheme shows graphs of transference X as a function of control current voltage U conducted to magnetic rheology throttles. The start voltage of the drive is $U_t = 0.21$ V that corresponds to the starting current $I_t = 0.014$ A. The form of the graph in Figure 6.19 shows the presence of $X = f(U)$ hysteresis (see schemes b and c in Figure 6.19). The controlling voltage in scheme c reaches its saturation zone at voltage $U = 2$ V and function $X = f(U)$. In this case it applies to the non-linear form of the graph.

For objects transference in small range (up to 1 mm) into three orthogonal coordinates X, Y, Z, it is possible to use a magnetic rheology manipulator [4], the scheme of which is shown in Figure 6.20. The manipulator contains a moving carriage 1, static base 2, rod 3 supplied with high pressure chambers, three pairs of magnetic rheology throttles 4 situated on input zone of high pressure chambers, bellow 5 and thin-wall rubber socks 6.

The manipulator works as follows. The work liquid (magnetic rheology suspension) is spilled through magnetic rheology throttles 4 into high pressure chambers of rod 3 and then it is spilled through the work gaps between the rod and the carriage to the output zone. By variation of control signal of magnetic rheology throttle it is possible to control the pressure of work liquid in chambers of high pressure and to transfer carriage 1 in three coordinates X, Y, Z. The drive is used for mirrors alignment in adaptive optical systems. The weight of the mirrors is almost 150 kg, error of transference is below 50 nanometers, quick-action (time constant) below 100 mil-

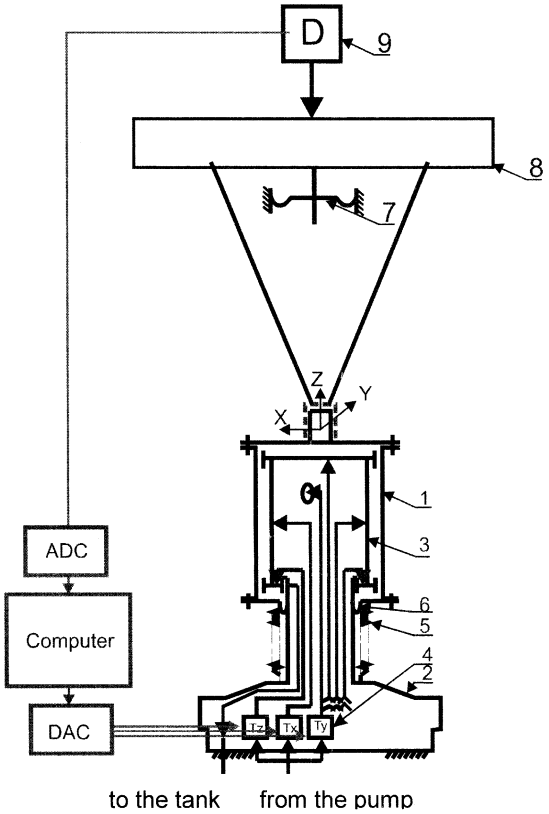

Fig. 6.20 Scheme of three coordinate tuning magnetic rheology drive.

liseconds [4]. The general view of the magnetic rheology manipulator is shown in Figure 6.21.

The equipment of microlithography, electron beam and X-ray lithography and synchrotron radiation require the object transference in three coordinates or more. Magnetic rheology manipulator (see scheme in Figure 6.22) can provide object transference in one long travel coordinate Z (travel range up to 200 mm) and in two coordinates X and Y (travel range up to 200 mic). It can also turn around axes X and Y (travel range up to 3 angular minutes) [11]

The drive contains hydro pump 1, static body 2 and moving cylinder rod. The drive is built in the form of hydrostatic way of the cylinder type supplied in a body 2 with four chambers of high pressure which form a basic element of a guide. To ensure the stability of moving cylinder rod the guide contains two basic elements fixed along axis Z. Magnetic rheology throttles in the input zone of the high pressure chambers are supplied with electromagnetic coils K1–K4, magnetic rheology throttles in the output zone are supplied with electro magnetic coils K6–K7 (coils

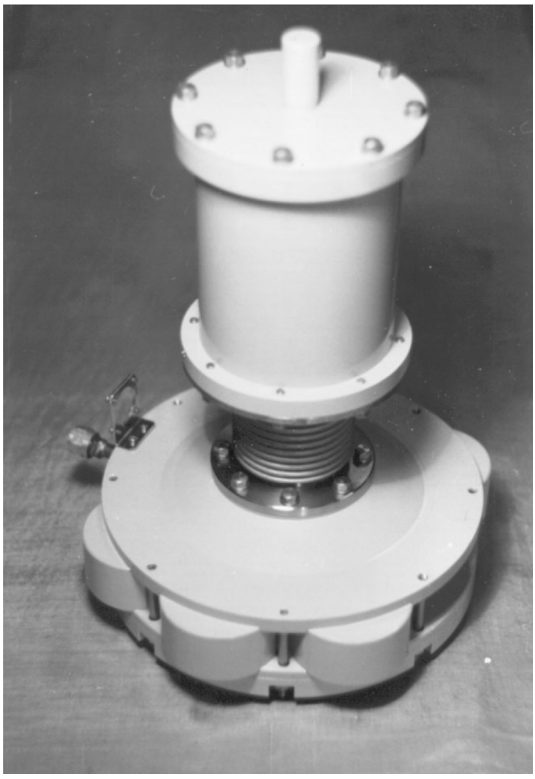

Fig. 6.21 General view of three coordinate tuning magnetic rheology drive.

K5–K7 are not shown). Magnetic rheology manipulator is sealed by thin-wall rubber socks. The drive works as follows: the work liquid (magnetic rheology suspension) is spilled from the tank by the pump 1 through magnetic rheology throttles supplied with electro-magnetic coils K1–K4. The work liquid is spilled into the high pressure chambers from the spillage tank and runs through radial work gaps between the cylinder rod and magnetic circuit of output magnetic rheology throttles supplied with coils which are supplied with coils K–5, K–8 and then it runs to the spillage tank. Using electrical current variation in coils of magnetic rheology throttles it is possible to vary pressure in the chambers of the drive. Therefore, the moving rod raises in the body 2 and the rod transfers along axes X and Y and is also transferred around axis Z by the long travel drive (this drive is not shown in the scheme). The general view of six-coordinate magnetic rheology drive based on hydrostatic guides and which is used for microlithography is shown in Figure 6.23.

The further idea of the use of magnetic rheology effect for vacuum mechanisms of nanoscale precision consists in the development of vacuum mechanisms based on the electric rheology effect. The electric rheology effect helps to increase the transference precision of the drive. It also helps to improve its dynamic parameters, to

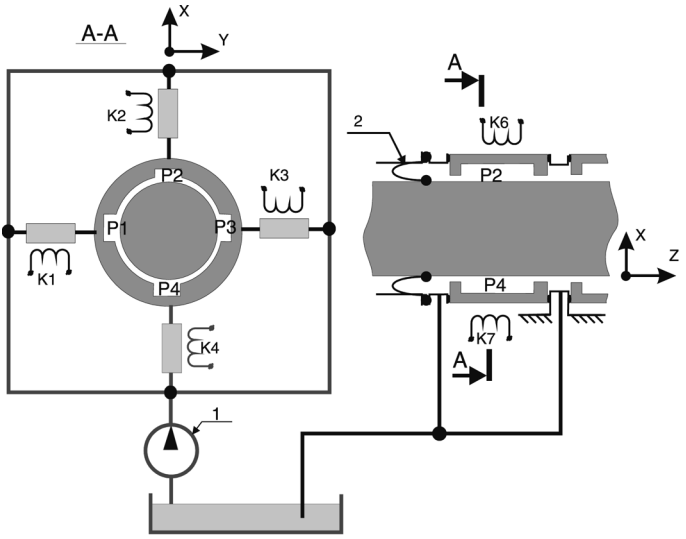

Fig. 6.22 Scheme of five coordinate magnetic rheology manipulator with long travel transference.

decrease its sizes and to decrease the weight of the vacuum mechanism. The main element of this drive is an electric rheology throttle (see Figure 6.24) which is realized in the form of a flat gap or in the form of a circular gap between metal surfaces supplied with a controlling high voltage. Variation of high voltage of electric field tension enables to vary dynamic viscosity of the work liquid (electric rheology suspension), which leaks through the gap. An electric rheology throttle allows one to exclude electromagnetic coils and to exclude magnetic circuits which are used in a magnetic rheology drive.

Let us consider a scheme of five coordinates – electric rheology manipulator [19] equipped with a loop-controlled system (see Figure 6.24). The manipulator contains input electric rheology throttles 1 and output electric rheology throttles 2, optical sensors of transference 3, control blocks 4. The manipulator is done in a form of hydrostatic guide of cylinder-shape. This guide is supplied with a static rod which contains chambers of high pressure and output electric rheology throttles 2. The mobile body with transferred object is sealed by of thin-wall rubber socks. The work liquid (an electric rheology suspension) is pumped by the pump through input electric rheology throttles 1 and through work radial gaps of output electric rheology throttles 2 and then into spillage tank. The control voltage of control block 4 is regulated on sockets of electric rheology throttles. This voltage of control block regulates pressure in the chambers of high pressure. The manipulator body rises in a layer of work liquid in the process of control. The manipulator body can be transferred in the direction of the X, Y, Z axes (in a range of up to 200 mm) and can be rotated around the axes X, Y (about 3 angular minutes). Let us estimate the components of total error of positioning $\delta\varphi_\Sigma$ (see Equation (5.10)) in case of magnetic

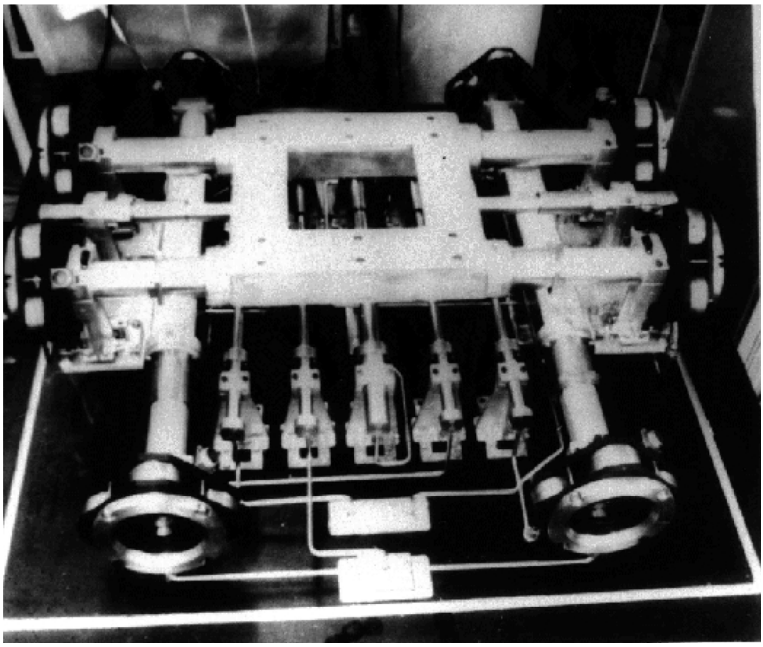

Fig. 6.23 General view of six coordinate magnetic rheology manipulator of microlithography installations.

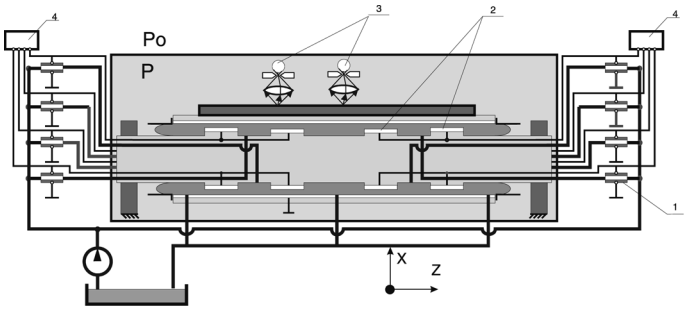

Fig. 6.24 Scheme of five coordinate electric rheology manipulator.

rheology manipulator with thin-wall socks (Figure 6.16). The transfer function of automatic loop control system of this manipulator can be estimated as

$$W_{\Pi}(S) = k_{\Pi}/(S(T_1S + 1)(T_2S + 1)), \tag{6.19}$$

where k_{Π} is the common gain factor (multiplication factor) of the drive; T_1, T_2 are the constant time factors of drive elements; S is the Laplace variable.

As we can see from Equation (6.19) the automatic control system of manipulator is a static automatic control system which contains one integrating chain element.

The error of driving action variation δ_V in the drive static control system (at level $\nu = 0$) is the drive error of driving action variation $\delta_V = C_0\varphi$. The drive static control system which contains one integrant element ($\nu = 1$) the positioning error is equal to zero ($C_0 = 0$).

Thus, as we can see from Equation (6.1), the positioning error is equal to zero and the error of driving action variation component depends on the speed dynamic error:

$$\delta_B = C_1\omega,$$

where ω is the stabilized speed of the drive linear transference along axis Z; C_1 is the speed error coefficient. This coefficient can be determined as

$$C_1 = 1/k, \tag{6.20}$$

where k is the common speed transmission coefficient of automatic control system of an automatically controlled drive. There is no acceleration current in this case. In case of magnetic rheology manipulator: $k = 6.282 \cdot 10^3$ 1/s and $C_1 = 1/(6.282 \cdot 10^3) = 1.59 \cdot 10^{-4}$ s.

In case of a stable transference of magnetic rheology manipulator at "small static speed", we have $\omega = 0.5 \cdot 10^{-4}$ m/s and the "component of speed dynamic error" is $\delta_V = 7.95 \cdot 10^{-9}$ m.

In case of disturbing forces (F_{dist}) (technology forces variation, vibration of base forces, variation in atmosphere pressure forces after the vacuum chamber is opening, energy variation and hydraulic pumping station variation) the error δ_N appears. This error depends on initial conditions.

Let us find this manipulator work error in case of manipulator work in positioning point. In this case all coils K1–K4 are supplied with maximal control current ($I = 1$ A) and all magnetic rheology throttles are closed. Error δ_N in this case depends of tubes rigidity. The tubes situate between magnetic rheology distributor and hydro-cylinders supplied with thin-wall rubber tubes. Error δ_N depends also on the work liquid, on tubes of hydro-cylinders and on thin-wall rubber tubes rigidity:

$$\delta_N = F_{\text{dist}} \cdot C_r / S_{\text{eff}}^2, \tag{6.21}$$

where C_r is the total coefficient of tubes rigidity, thin-wall rubber elements, work liquid rigidity; S_{eff} is the effective area of thin-wall rubber elements in hydro-cylinders. So, in the case of disturbing forces (F_{dist}) (technology forces variation, vibration of base forces, atmosphere pressure forces variation after the vacuum chamber opening, energy variation and hydraulic pumping station variation) the error is equal to $\delta_N = 0.1 \cdot 1.342 \cdot 10^{-14}/(4.9 \times 10^{-4})^2 = 5.59 \cdot 10^{-9}$ m. The error caused by static friction forces in the manipulator can be expressed by Equation (5.13) and in the case of resistance force $F_{TP} = 0.05$ N it is equal to

$$\delta_c = 0.05/10^6 = 5 \cdot 10^{-8} \text{ m}.$$

Recoil error δ_L in magnetic rheology manipulator is equal to zero. In case of using a laser interferometer the instrumental error is equal to $\delta_I = 10^{-8}$ m. The total error of positioning is equal to $\delta\varphi_\Sigma = (7.95+5.59+50+10)\cdot 10^{-9} = 73.54\cdot 10^{-9}$ m and a magnetic rheology manipulator of this precision can be used for previous ("rough") transference of objects. Analysis of precision, dynamic and vacuum parameters of precise vacuum manipulators performed in Sections 6.1–6.3, shows that vacuum manipulators with the highest parameters are the vacuum manipulators based on piezo transformers and the manipulators of hydraulic type based on magnetic rheology and electric rheology effects. Piezo tubes allows one to transfer objects in ultrahigh vacuum ($p \leq 5 \cdot 10^{-8}$ Pa) with error of positioning less than 0.1 nm in the range of transference of up to 100 mic.

Magnetic rheology manipulator and electric rheology manipulator can be used to transfer objects in high vacuum and in ultrahigh vacuum ($p \leq 5 \cdot 10^{-8}$ Pa); in large ranges of transference of up to 200 mm, and to ensure an error of positioning less than 10 nm. They have good dynamic parameters: the time constant of a magnetic rheology drive is less than 100 milliseconds, the time constant of an electric rheology drive is less than 1 millisecond. They also have good damping parameters.

References

1. Landberg E.E., Mrrja C.L., Hewlett Packard, No. 5, 1981, pp. 16–18.
2. Wilson A.D., *Solid State Technol.* **29**(5), 1986, 249–255.
3. Eltsov K.N., Klimov A.N., Priadkin S.L., Shevlyuga V.M., Yurov V.Y., *Phys. Low-Dim. Struct.* **7/8**, 1996, 115–126.
4. Deulin E.A., Mikhailov V.P., Eliseev O.N., Sytchev V.V., *Proceedings of SPIE* **4003**, 2000, 303–310.
5. Smirnova V.I. et al., *The Base of Design and Calculation of Computer Regulated Drives*, Mashinostroenie, Moscow, 1983, 285 pp.
6. Ivashenko N.N., *Automatic Control*, Mashinostroenie, Moscow, 1978, 608 pp. [in Russian].
7. Makarov I.M., Menski B.M., *Linear Automatic Systems*, Mashinostroenie, Moscow, 1982, 504 pp. [in Russian].
8. Ichibara S., *Bull. Japan Soc. of Precision Engineering* **21**(1), 1987, 1–8.
9. Ravva J.S., *New Decision in Lathes Precision Increasing. Adoptatation of the System with Complex Friction*, Knijnoe Izdatelstvo, Kuibushev, 1974, 214 pp.
10. Deulin et al., *Vacuum* **44**(5–7), 1993, 469–470.
11. Anisimov V.V. et al., *Vacuum* **47**(10), October 1996, 1163–1165.
12. Panfilov Y.V., Ryabov V.T., Tsvetkov Y.B., *Equipment for Integral Schemes Manufacturing*, Radio and Sviaz, Moscow, 1988, 320 pp. [in Russian].
13. Chen V.K., *Journal of Physics* **11**(1), 1978, 1092–1093.
14. *The Power of Precision in Nanopositioning*, Burleigh Instruments, Inc. Burleigh Park, Fishers, NY 14453-0755, USA, 1997.
15. Yaffe B.I., *Piezo Electric Ceramic*, Mir, Moscow, 1974, 288 pp. [in Russian].
16. Shulman Z.P., Kordonski V.I., *Magnetic Rheological Effect*, Nauka and Technika, Minsk, 1982, 184 pp. [in Russian].
17. Bibik E.E., Some effects of microparticles mitual action in a process of ferrum liquid flow in magnetic field, *Magnetic Hydrodynamic* **3**, 1973, 25–32 [in Russian].
18. Bashta T.M., *Machine Building Machines*, Mashinostroenie, Moscow, 1971, 672 pp.
19. Anisimov V., Deulin E.A., Mikhailov V.P., Kasperski V., Sytchev V.V., *Proceedings of SPIE* **2871**, 1996, 641–648.